Growth of magnetic cobalt/chromium nano-arrays by atom-optical lithography

2011 J. Phys.: Conf. Ser. 303 012046

(http://iopscience.iop.org/1742-6596/303/1/012046)

Joint European Magnetic Symposia – JEMS 2010 IOP Publishing
Journal of Physics: Conference Series **303** (2011) 012046 doi:10.1088/1742-6596/303/1/012046

Growth of magnetic cobalt/chromium nano-arrays by atom-optical lithography

F. Atoneche, D. Malik, A. Kirilyuk, A. J. Toonen, A. F. van Etteger, and Th. Rasing

Radboud University Nijmegen, Institute for Molecules and Materials, Heyendaalseweg 135, 6525 AJ, Nijmegen, The Netherlands

E-mail: f.atoneche@science.ru.nl

Abstract. Arrays of magnetic cobalt/chromium (Co-Cr) nanolines are grown by depositing an atomic beam of Co-Cr alloy through a laser standing wave (SW) at $\lambda/2 = 212.8$ nm onto a substrate. During deposition, only the chromium atoms are resonantly affected by the optical potential created by the SW, causing a periodic modulation of the chromium concentration and consequently of the magnetic properties. Magnetic force microscopy and magneto-optical Kerr effect studies reveal a patterned magnetic structure on the substrate surface.

1. Introduction

The fabrication and characterization of micro- and nano-structured magnetic dots and arrays is an area of intense research [1, 2, 3] in recent years. Their main interest stems not only from their importance as model systems for the study of magnetic interactions, including coupling and ordering phenomena [3], but also from their potential for the development of future storage devices. Different techniques (most of them involving two-steps or more) like electro-deposition, the very slow electron beam lithography process, and anisotropic etching of substrates, have been implored for the fabrication of these arrays. Despite all these efforts, a one-step process for the fabrication of magnetic arrays remained a challenge.

Here we present such a one-step technique of fabricating magnetic nanostructures via atom-optical modulation of the concentration of a binary alloy, demonstrating a new method of nanoscale modulated magnetic material composition. The advantage of this technique is that it offers inherent parallelism and ultrahigh vacuum compatibility, with unrivaled periodicity [4].

The method is based on the interaction of a thermal atomic beam with a slightly detuned resonant laser standing wave (SW) resulting in a direct optical manipulation of atoms as described in [5]. By using a combination of laser beams, various structures can be created, such as nanowires and nanodots with 2, 3, 4 or even 5-fold symmetry [6]. Iron nonowires grown in this way however showed no periodic magnetic behavior [5], presumably because of a large background layer.

In this study, we utilize the simultaneous deposition of chromium and cobalt atoms through a spatially varying optical SW potential (for Cr) to create a concentration modulated alloy structure on a silicon substrate. During deposition, selective manipulation of chromium is achieved by using a laser wavelength (of 425.55 nm) that is near resonant with the ^{52}Cr transition $^7S_3 \rightarrow {}^7P_4^0$ while Co is uniformly deposited. Because the magnetic properties of

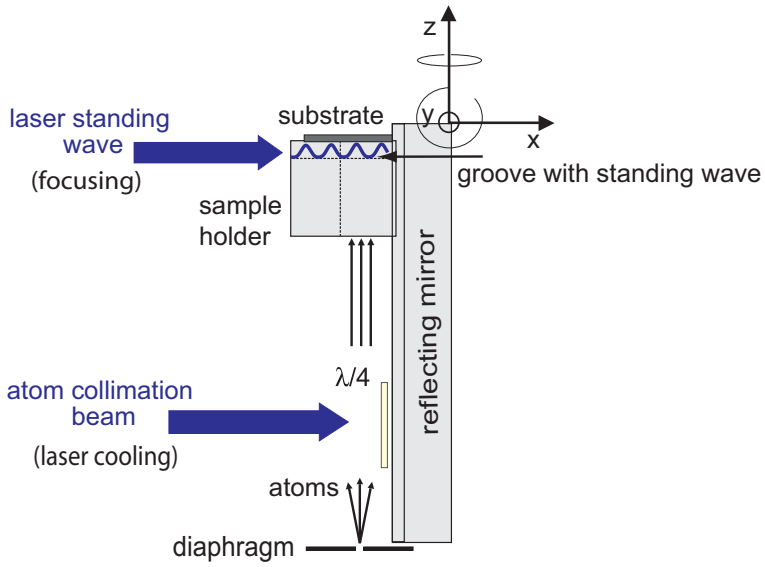

Figure 1. (color online) *In vacuo* optics showing substrate and positions of atom collimation beam and laser standing wave. The required degrees of freedom of the manipulator in x, y and z are also shown.

Co-Cr strongly depend on the Cr concentration, and by carefully selecting the concentration in the starting alloy material, this results in a uniform array of nanolines revealed by atomic force microscopy studies, with periodically varying magnetic properties observable in magnetic force microscopy. The period is 212.8 nm and the full width at half maximum (FWHM) is 90 nm. MOKE measurements reveal a uniaxial anisotropy parallel to the lines and a vanishing saturation magnetization perpendicular to the lines.

2. Experiment

For the experiment, blue continuous wave (CW) laser light at 425.55 nm was obtained by frequency doubling the output of a titanium-doped sapphire ring laser in an external enhancement cavity fitted with a lithium triborate (LBO) crystal [7]. For the deposition, we used a beryllium oxide crucible holding a Co-Cr alloy of composition Co-86/Cr-14 wt percent and particle size of $\leq$ 150 μm. The alloy composition was carefully chosen so that, in the alloy form, the mixture would still be magnetic [8]. We also note that evaporation of the alloy constituents at the same temperature should also be possible. In order to evaporate the alloy for deposition, a high temperature effusion cell holding the crucible with the alloy was heated up to a temperature of 2030 K. This assembly, below called the oven, produced a thermal beam of neutral chromium and cobalt atoms. The base pressure in the deposition chamber is routinely below 10^{-8} mbar and around 10^{-7} mbar during deposition. The thermal beam was collimated by means of transverse laser cooling, after it had gone through a defining diaphragm of 0.7 mm diameter. The power in the cooling beam was 55 mW. Its frequency was tuned by about 10 MHz below the Cr resonance, allowing for the atoms to only lose energy and momentum by scattering of the laser light [9]. The atomic beam could be transversally collimated to a divergence angle of 0.6 $\pm$0.1 mrad FWHM. It was then deposited on a silicon substrate through a one-dimensional SW potential. An *in vacuo* optical alignment unit shown in Fig. 1, could be rotated around the y and z axes and included translations in the x-, y- and z-directions. The mirror was made of a zerodur substrate coated with aluminum. The sample rested on the top part of a sample holder

cut from a prism. Two grooves were cut into the holder in the x- and z directions for the laser SW and atom beam respectively.

The SW laser frequency was tuned approximately 200 MHz above the ^{52}Cr transition $^7S_3 \rightarrow ^7 P_4^0$ at 425.55 nm using an acousto-optic modulator. The positive detuning causes the atoms to be focused to the intensity minima (nodes) of the SW [10]. The power in the SW was 30 mW focused to $W_0 = 200$ μm. The optical unit (Figure 1) was then moved into position so that the vertical atomic beam was directed into the groove and through the SW. The substrate was then moved down to the center of the standing wave. We note here that only the chromium atoms are affected by the light. The deposition time was 30 minutes.

3. Results and Discussion

We studied the fabricated samples *ex vacuo* by atomic force microscopy (AFM), magnetic force microscopy (MFM) and the magneto-optical Kerr effect (MOKE). Figure 2(a) shows an AFM picture of an array of periodic nanolines with a height above background (film formed from atoms not focused by the SW) of 3 nm. Note that the background film thickness was determined by ellipsometry to be 10 $\pm$ 0.04 nm. This gives a height to background ratio of $\approx 1:3$. The periodicity is 212.8 nm which is that of the interference pattern created by the standing wave laser beam at 425.55 nm. Notice an obstacle (probably dirt particle) on the surface of the sample. Figures 2(b,d) show a zoomed-in AFM and an MFM picture of the obstacle, respectively. While no topographic contrast is visible through this round obstacle (Figure 2(b)), the MFM image, of the same area as in the AFM picture, taken at a lift height of 30 nm, shows a clear magnetic contrast. (Figure 2(d)).

In the phase detection scheme of MFM, changes $\Delta\phi$ in the phase shift of the cantilever's phase oscillation relative to a piezo drive are measured. If a force F acts on the cantilever in the opposite direction to the vibration direction z, then the changes in the phase shift can be expressed as [11]:

$$\Delta\phi \approx -Q/K(\partial F/\partial z), \tag{1}$$

where K is the cantilever spring constant and Q is the quality factor of the vibrating system. For an attractive force, the force gradient, $\partial F/\partial z > 0$. This leads to a negative phase shift, $\Delta\phi$. The negative phase shift means that the phase ϕ is reduced, corresponding to a darker contrast. For a repulsive force, $\partial F/\partial z < 0$, leading to an increase in the phase which corresponds to a bright contrast.

The MFM measurements shown in Figures 2(c) and (d) fit the description of standard MFM behavior above, as the dark contrast regions are magnetic and correspond to regions where an attractive interaction exists between the sample and the tip. In our sample, the ridges have higher chromium concentration due to the focused chromium atoms. A higher Cr concentration leads to non magnetic ridges. On the other hand, the valleys have a higher concentration of cobalt since most of the chromium atoms are directed away from these regions by the laser standing wave pattern. The result is a magnetic contrast between the magnetic valleys and non-magnetic ridges, revealed by MFM imaging.

In order to further characterize the magnetic properties of the nanolines, static longitudinal MOKE measurements were performed using a HeNe laser polarized perpendicular to the plane of incidence. The inset of Figure 3(a) shows a schematic picture of the experimental layout. The laser beam was focused to a spot size of 40 microns. This allowed for a good spatial resolution to obtain a signal related to the structured region of the sample only. Figure 3(a) shows MOKE measurements at different positions, 1, 2 and 3, across the sample for $\phi = 0\circ$. No magnetic signal was observed at position 1, where the Co-Cr film is homogeneous. This was further confirmed by the non saturation of the magnetization in this region even at fields as high as 0.2 kG. This means that during the deposition, a higher percentage of Cr than contained in the original material, might have been evaporated. This can be explained by a higher Cr vapour pressure

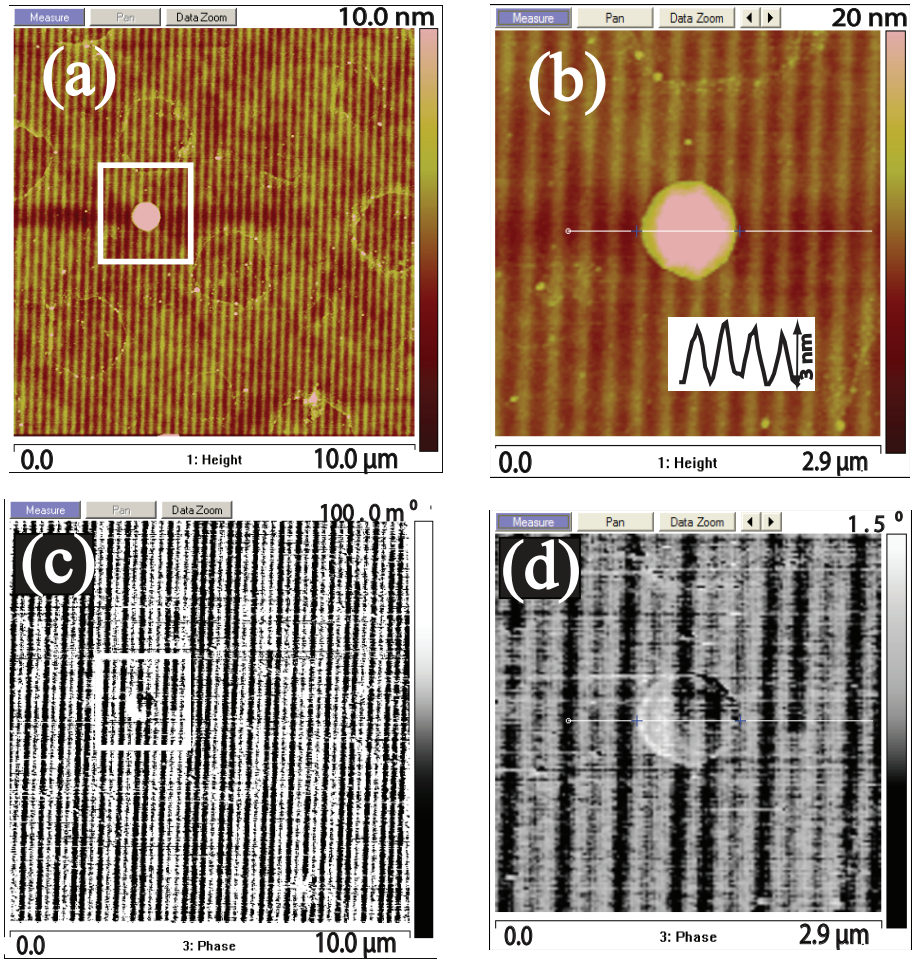

Figure 2. (color online)Laser-focused Co-Cr nanolines a) Patterned Co-Cr alloy lines as observed by AFM. b) zoom in showing area enclosed by rectangle in (a). c) MFM image. d) shows enclosed area in (c) with magnetic contrast visible under round spot in middle. Black areas are magnetic and white areas are non-magnetic.

at the evaporation temperature [12]. At position 2, on the edge of the modulated area, a weak magnetic contrast can be observed which further increases towards the center of the nanolines (position 3).

The sample could also be rotated around an axis perpendicular to its surface, leading to a variation of the angle ϕ of the applied field with respect to the direction of the nanolines.

Figure 3(b) shows MOKE hysteresis loops measured for different orientations ϕ of the applied magnetic field, relative to the nanolines. The maximum Kerr rotation is observed when $\phi = 0°$. In this case the hysteresis loop is almost square-like. This behavior is characteristic of a specimen magnetized to saturation along an easy axis. For this case, the saturating field is about 0.2 G. Increasing the angle ϕ leads to a smaller Kerr rotation which disappears completely for $\phi = 90°$. The inset of Figure 3(b) shows a plot of the Kerr angle θ_k at magnetization saturation, normalised by the maximum Kerr angle θ_m, at parallel alignment (ϕ=0°) as a function of the angle ϕ. The normalized Kerr rotation at magnetization saturation decreases with increasing ϕ. The magnetization saturation and coercivity fields are extremely low compared to typical large saturation fields and coercivities of thin film Co-Cr alloys of comparable thickness [14]. Note

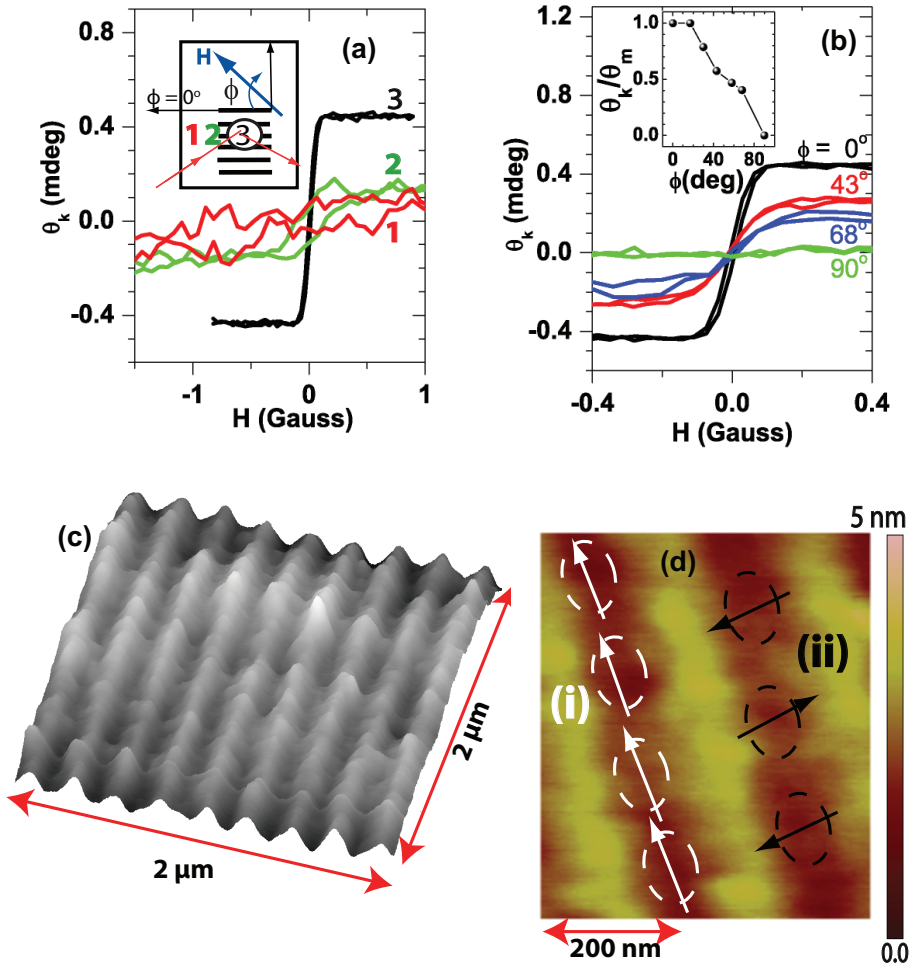

Figure 3. (color online) Inset of a) schematic picture of the sample for MOKE measurements. a) Hysteresis loops across the sample for ϕ=0°. b) Hysteresis loops measured for different angles ϕ. Inset of b) Normalized plot of Kerr angle θ_k, at saturation as a function of ϕ. c) High resolution 3D AFM image showing disconnected "droplets". d) AFM image showing disconnected magnetic "droplets" and alignment scenario in parallel field (i), and in perpendicular field (ii).

that the earth's magnetic field was compensated for during deposition and ex-vacuo magneto optical studies. We observe not just an increase of the saturation field, as is expected when going from the easy- to the hard magnetization axis. In addition, the saturation magnetization vanishes, which was also verified by increasing the applied magnetic field range up to 0.4 kG. Therefore, the patterned area exhibits an anisotropy parallel to the nanolines. This effect is nontrivial and cannot be explained by treating the nanolines as being fully continuous. We can explain this behavior by assuming that our nanolines consist of small magnetic "droplets" that are magnetostatically coupled to each other. A strong argument for the presence of such a non-continuous structure is given by the MFM picture: Moreover, if the nanolines were continuous, no contrast in the MFM images would be observed at all because stray fields "felt" by the MFM tip would only be present at the ends of the nanowires. Figure 3(c,d) appears to reveal these magnetic "droplets". The coupling is ferromagnetic if the magnetization is along the "droplets" chain. Rotating the magnetization by 90° changes the coupling to antiferromagnetic, destroying

the net magnetization of the chain. Note that given the subtle balance of Co-Cr concentration ratio, the formation of such magnetic droplets is quite probable.

The results of magnetic characterization presented above only provide a qualitative understanding of the magnetic properties of the concentration modulated patterned nanolines on the substrate. Moreover, although the composition of the alloy is carefully chosen before evaporation, that of the material deposited on the substrate is largely unknown because of the uneven evaporation of Cr and Co due to the difference in their vapor pressures at the evaporation temperature, and the vacuum conditions during evaporation. Therefore a further quantitative analysis of the observed magnetic behavior cannot be made without further studies, such as compositional analysis.

4. Conclusions

In conclusion, we fabricated Co-Cr magnetic nanostructures by modulating the concentration of chromium in a Co-Cr alloy via atom-optics at the nanoscale, thus demonstrating the proof-of-principle of a new method for nanoscale-modulated magnetic material composition. AFM investigations show a global periodic pattern of lines with a period of 212.8 nm and a height above the background of 3 nm while detailed MFM and MOKE studies reveal an alternating pattern of magnetic and nonmagnetic nanolines. Concentration modulation of an alloy constituent via atom-optics for nanofabrication is therefore a valid technique for the production of periodic magnetic nanostructures. By extending this method to 2-dimensional patterns [15], magnetic nanostructures with a variety of symmetries can be produced.

Acknowledgments

This work was supported by the Dutch organization for Fundamental Research on Matter (FOM), the NanoNed consortium and NWO.

References

[1] Mallet J, Yu-Zhang K, Chien C, Eagleton T S, and Searson P C 2004 Appl. Phys. Lett. **84**, 3900
[2] Choi J, Oh S J, Ju H, and Cheon J 2005 Nano Letts. **5**, 2179
[3] Wang Z K, Kuok M H, Ng S C, Lockwood D J, Cottam M G, Nielsch K, Wehrspohn R B, and Gsele U 2002 Phys. Rev. Lett. **89**, 027201
[4] McClelland J J, Scholten R E, Palm E C, and Celotta R J 1993 Science **262**, 877
[5] Myskiewicz G, Hohfeld J, Toonen A J, van Etteger A F, Shklyarevskii O I, Meerts W L, and Rasing Th 2004 Appl. Phys. Lett. **85**, 3842
[6] Jurdik E, Myszkiewicz G, Hohlfeld J, Tsukamoto A, Toonen A J, van Etteger A F, Gerritsen J, Hermsen J, Goldbach-Aschemann S, Meerts W L, van Kempen H, and Rasing Th (2004) Phys. Rev. B **69**, 201102,
[7] Jurdik E, Hohlfeld J, van Etteger A F, Toonen A J, Meerts W L, van Kempen H, and Rasing Th 2002 J. Opt. Soc. Am. B **19**, 1660
[8] Maeda Y, Asahi M and Seki M 1986 Jpn. J. Appl. Phys. **25**, L668
[9] Hansch T W and Schawlow A L 1975 Optics Comm. **13**, 68
[10] McClelland J J and Sheinfein M R 1991 J. Opt. Soc. Am. B **8**, 502
[11] Hartmann U 1999 Annu. Rev. Mater. Sci. **29**, 53
[12] Lide D R (ed) 2003 CRC Handbook of Chemistry and Physics, 84th Edition, CRC Press, Boca Raton, Florida, Section 6, Fluid Properties; Vapor Pressure.
[13] Theis-Brohl K, Schmitte T, Leiner V, Zabel H, Rott K, Brukl H and McCord J 2003 Phys. Rev. B **67**, 184415
[14] Yamamoto S, Wada H, Kurisu H and Matsuura M 2001 J. Magn. Magn. Mater. **235**, 133
[15] Bradley C C, Anderson W R, McClelland J J, and Celotta R J 1999 Appl. Surf. Science **141**, 210